Electronic Supplementary Material (ESI) for Journal of Materials Chemistry C.

Supporting Information for

Highly Sensitive Mechano-Optical Strain Sensor Based on 2D Material for Human Gaits Quality Monitoring and High End Robotic Applications

Haris Khan[a], Afaque Manzoor Soomro[b,*], Abdul Samad[a], Irfanullah[a], Muhammad Waqas[a,*], Hina Ashraf[c], Saeed Ahmed Khan[a], Kyung Hyun Choi[b]

[a]*Department of Electrical Engineering, Sukkur IBA University, Pakistan,*
[b]*Department of Mechatronics Engineering, Jeju National University, Republic of Korea,*
[c]*Department of Ocean Science Engineering, Jeju National University, Republic of Korea*
**Correspondence and request for materials should be addressed to Muhammad Waqas & Afaque Manzoor Soomro (Email addresses: mwaqas@iba-suk.edu.pk; afaquemanzoor@gmail.com)*

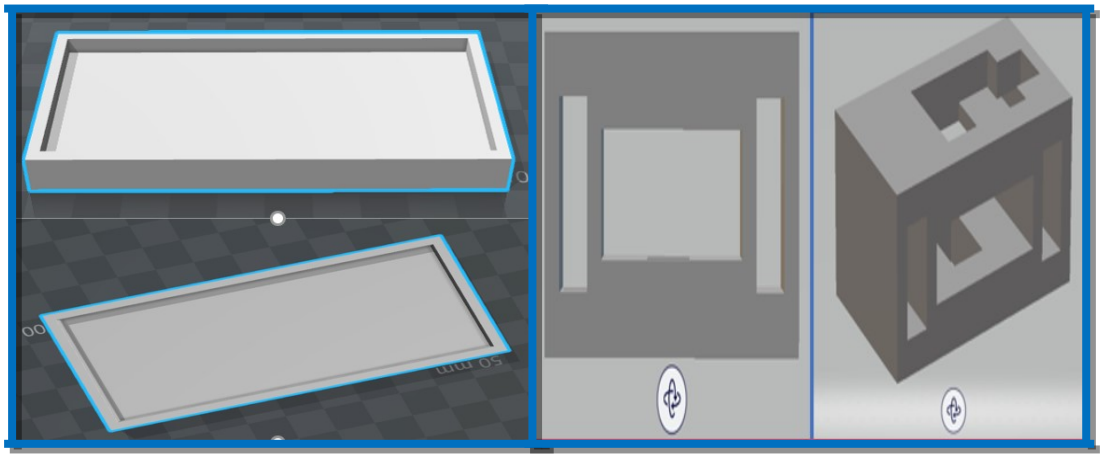

Fig. S1 (a) Design of casing for molding and casting of composite film **(b)** Design of LED-LDR assembly package.

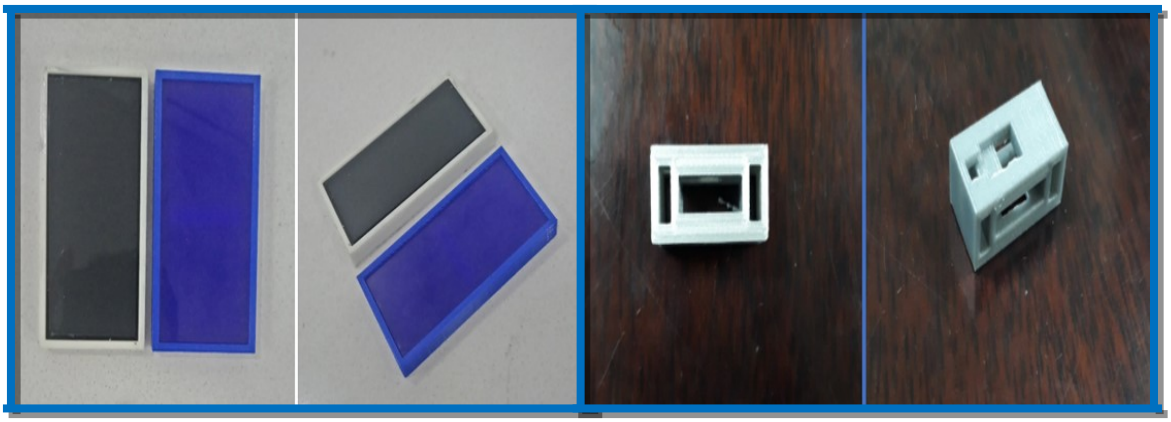

Fig. S2 Real-time images showing the: **(a)** 3D printing of casing for molding and casting of Ecoflex/MoS_2 composite film **(b)** 3D design of LED-LDR assembly package.

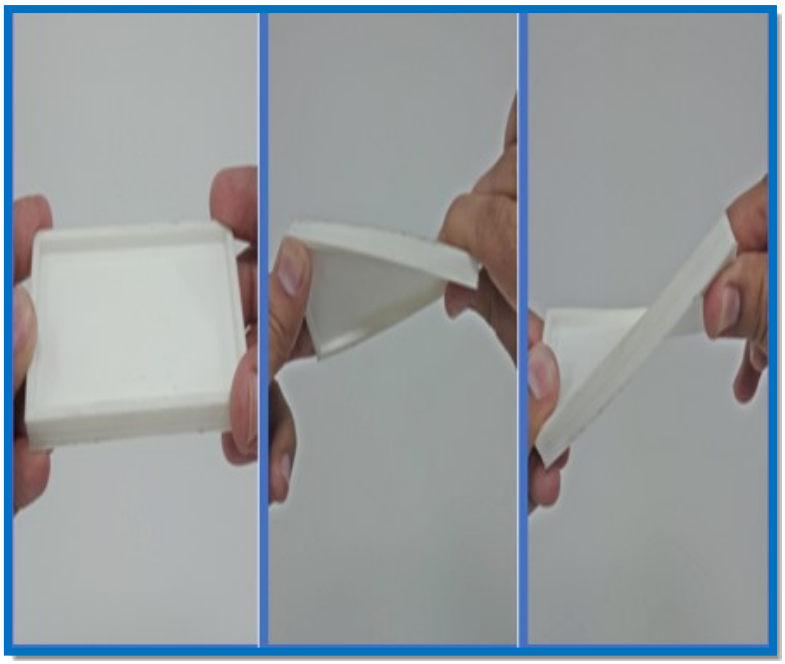

Fig. S3 Real-time images showing the flexibility of 3D printed casing for molding and casting of Ecoflex/MoS_2 composite film.

Fig. S4 Real-time images showing the casting of Ecoflex/MoS_2 composite film.

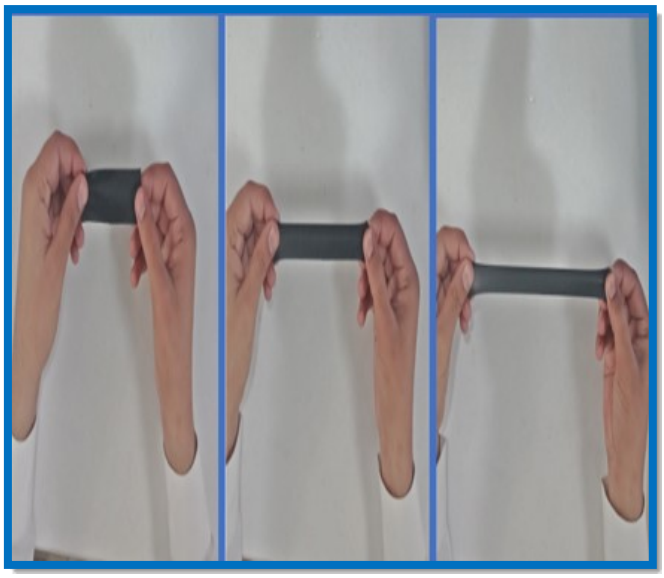

Fig. S5 Real-time images showing the manual stretching capability of Ecoflex/MoS_2 composite film.

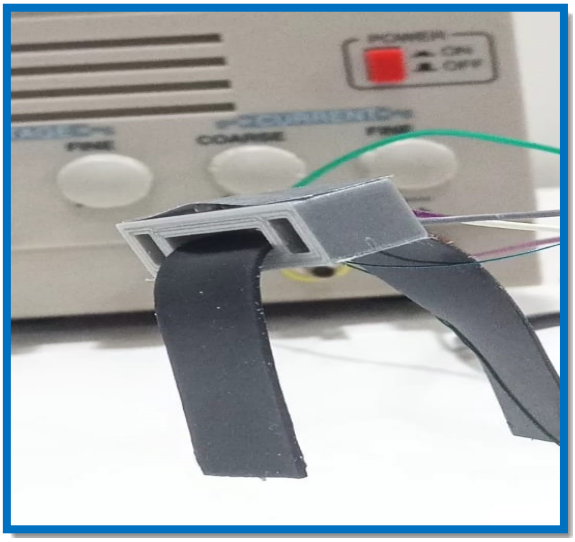

Fig. S6 Real-time images depicting the fabrication of a single sensor package based on Ecoflex/MoS_2 composite film and LED-LDR arrangements.

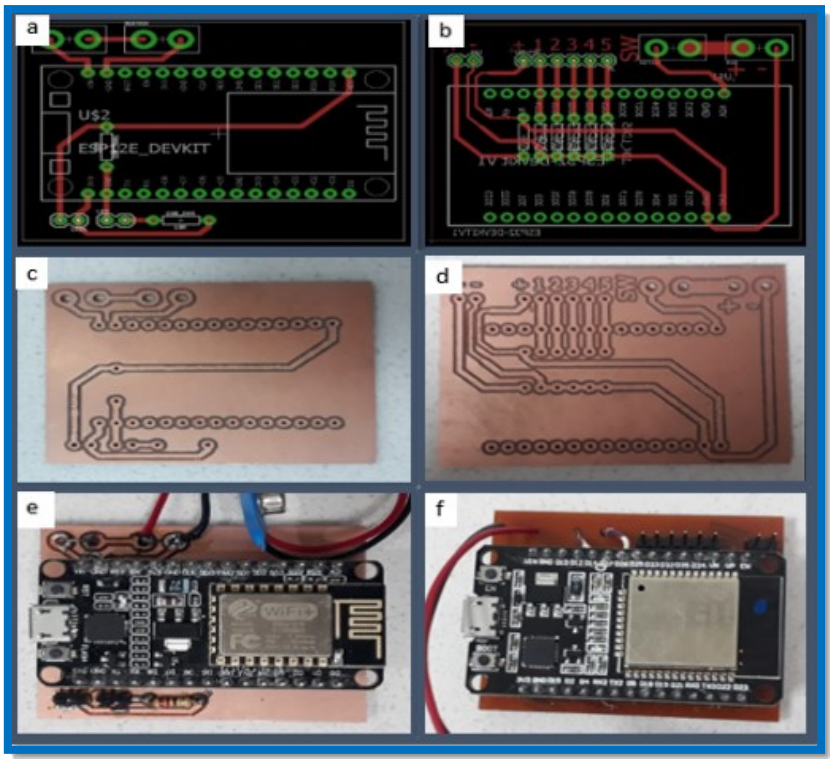

Fig. S7 (a, b) PCB design of hardware circuity, **(c, d)** Printed PCB boards, and **(e, f)** real-time images of complete hardware circuitry for the acquisition of sensor data and remote monitoring.

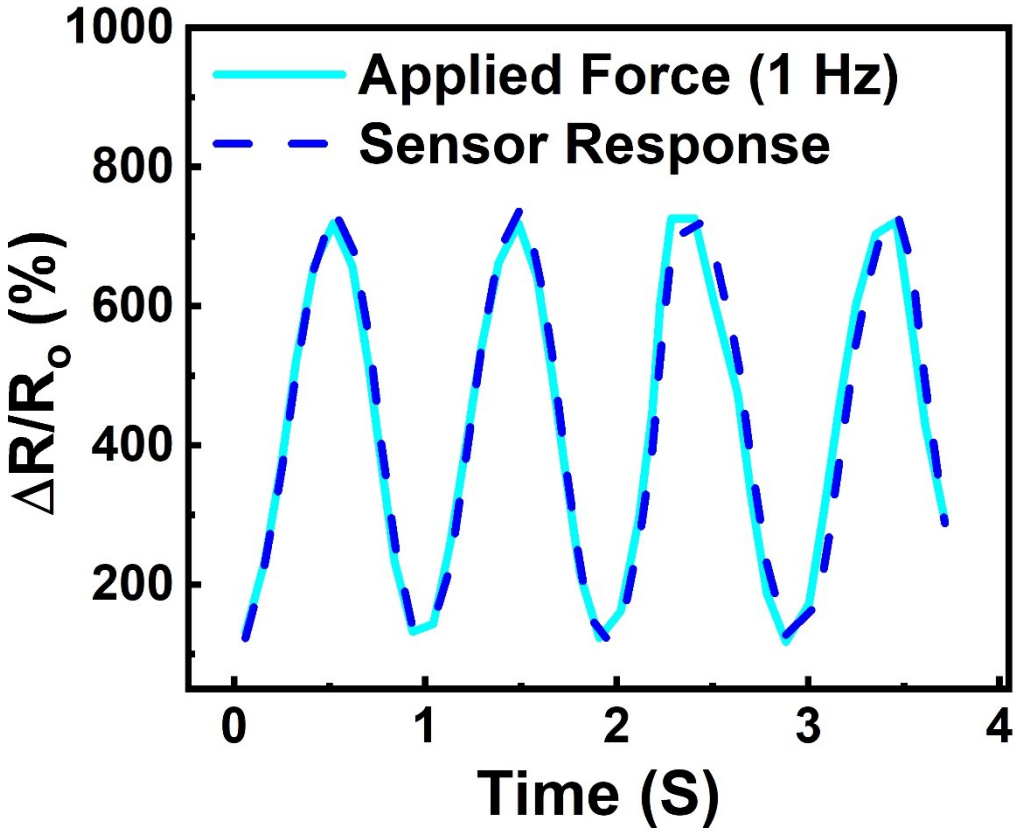

Fig. S8 Sensor response under uniaxial stretching at the rate of 1 Hz.

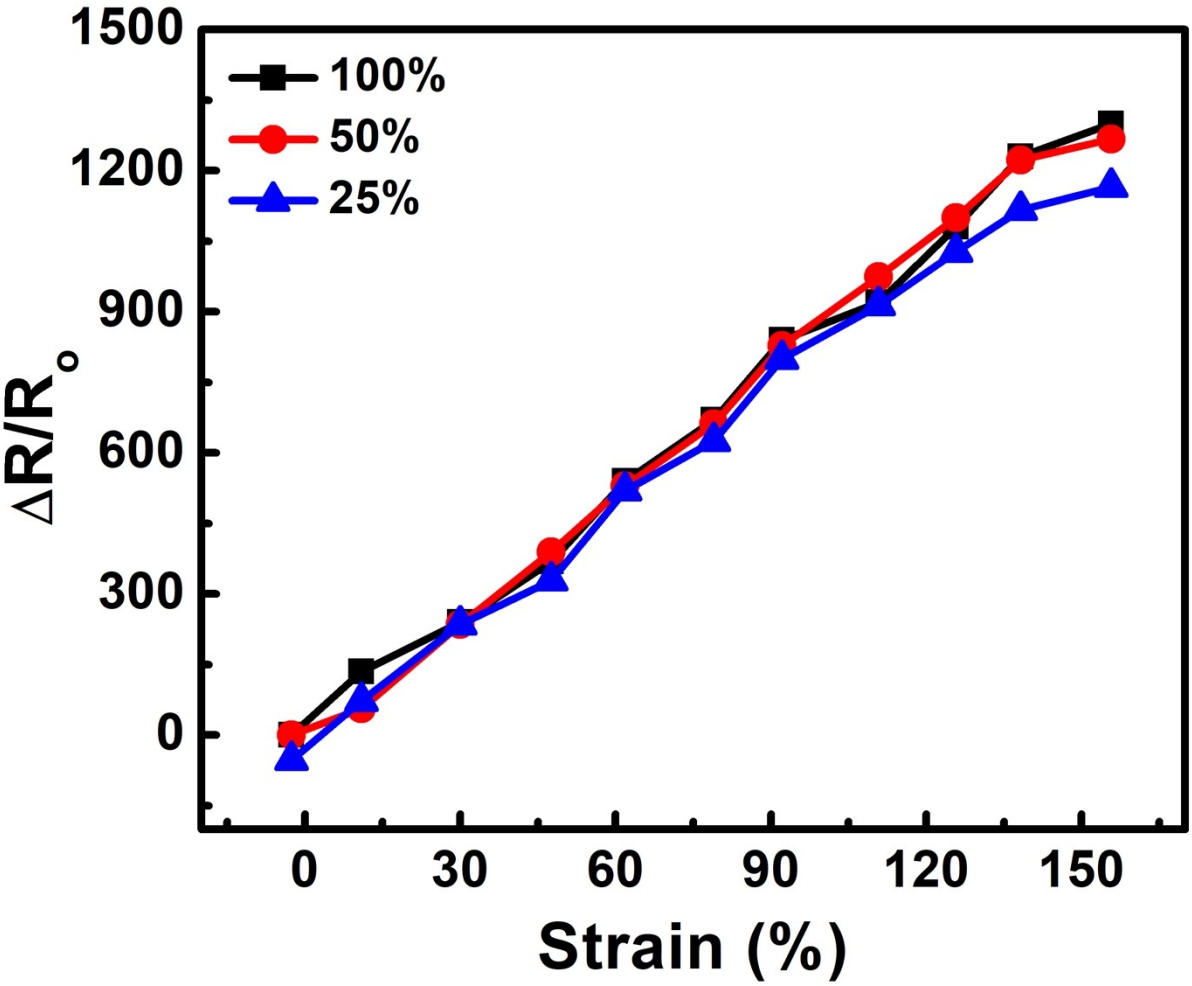

Fig. S9 Sensor's response when the LED is placed at different focus areas (25%, 50%, and 100%)

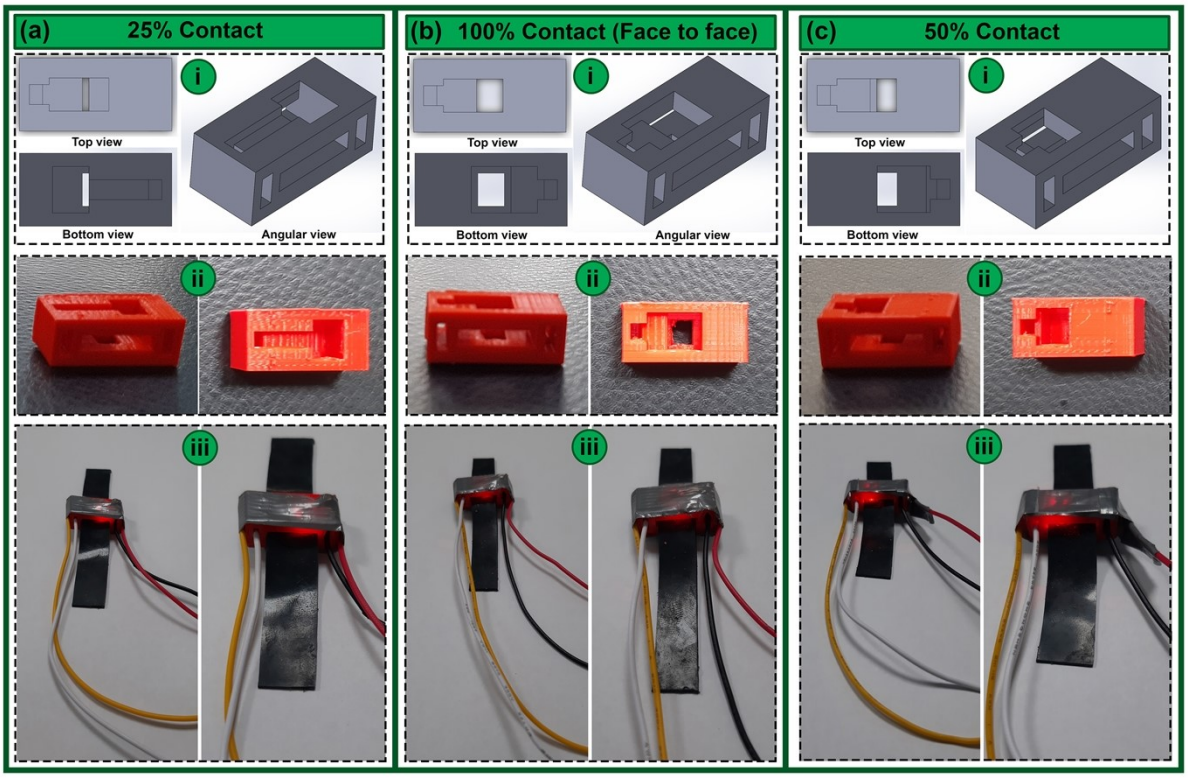

Fig. S10 (**a)** Shows the 3D drawing of the case with 25% focus area covered and its setup, (**b)** with 100% focus area, and (**c)** 50% focus area.

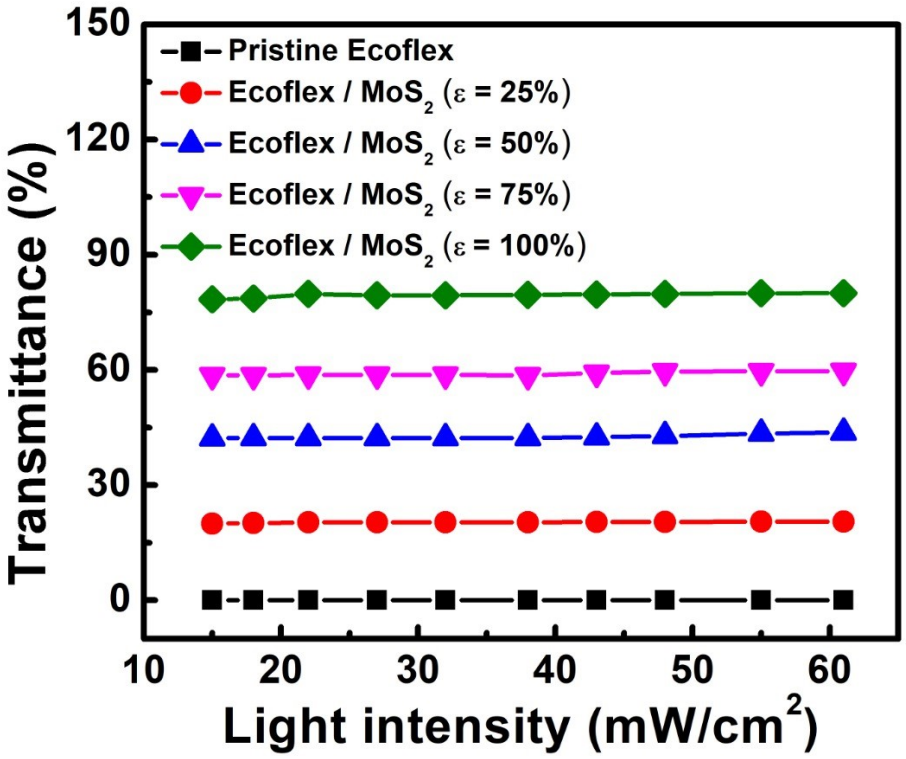

Fig. S11 Optical transmittance of the pristine Ecoflex and Ecoflex/MoS_2 when light intensity in the range of 12.5 – 52 mW/cm^2 was used.

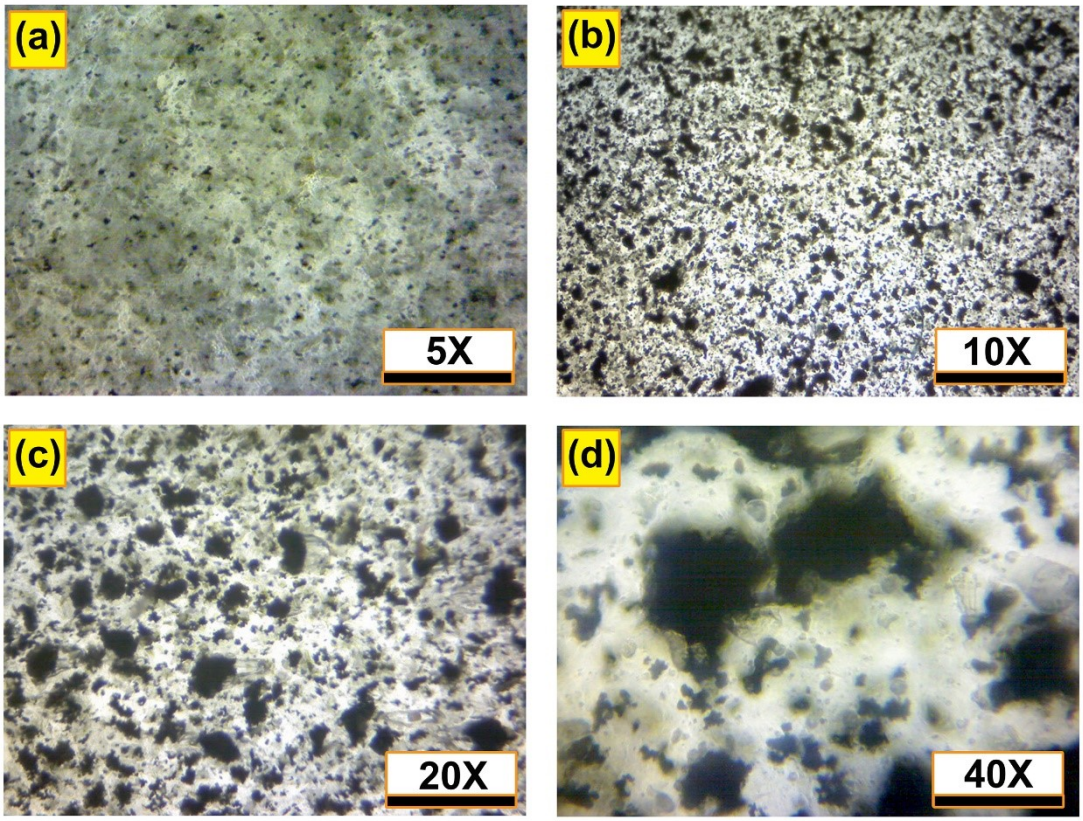

Fig. S12 microscopic images of the prepared membrane under different magnification levels (5X, 10X, 20X, and 40X).

Table S1 Comparison of performance parameters of the proposed device with reported devices

Sensing Material	Matrix Material	Sensing Range	Strain Frequency	DH (%)	GF	Cycles	COD	Technique	Ref.
GO-doped PU@PEDOT c	PU	550%	--	--	10.1	10000	--	Piezo Type	[1]
GaInSn	PDMS	50%	--	--	--	20	Almost linear	Liquid type	[2]
CNT	PDMS	300%	--	--	6.6	10000	0.9999	Piezo Type	[3]
NaCl-Ecoflex	Ecoflex	50%	--	21.34%	--	--	~0.999	Liquid type	[4]
Carbon grease solution	Ecoflex	100%	--	9.04%	3.8	1000	Non-linear	Liquid type	[5]
multi-walled CNTs	PDMS	60%	--	--	1.16	255	Non-linear	Piezo Type	[6]
KI-Gly	Ecoflex	50%	2 Hz	5.3%	2.2	4000	Almost linear	Liquid type	[7]
Ethylene glycol/NaCl	Ecoflex	250%	--	6.52%	<4	3000	~0.989	Liquid type	[8]
PEDOT: PSS	PDMS	30%	--	~9%	12,000	--	--	Liquid type	[9]
Graphene/ Glycerine	Ecoflex	1000%	--	--	45	10,000	Almost linear	Liquid type	[10]
CNTs	Ecoflex	100%	--	1.8%	30	--	0.98	Piezo Type	[11]
rGO/DI	Ecoflex	400%	--	31.6%	--	--	Almost linear	Liquid type	[12]
KCL-Gly	Ecoflex	100%	5 Hz	4.23%	2.7	8000	~0.99	Piezo Type	[13]
PEDOT:PSS/MWCNT	Ecoflex	150%	10 Hz	1.56%	89.4	1000	0.99	Liquid type	[14]
MOS_2	Ecoflex	150%	5 Hz	0.43%	8.6	1000	0.998	Optical Type	This work

1 K. Qi, J. He, H. Wang, Y. Zhou, X. You, N. Nan, W. Shao, L. Wang, B. Ding and S. Cui, *ACS Appl. Mater. Interfaces*, 2017, **9**, 42951–42960.

2 A. Nakamura, T. Hamanishi, S. Kawakami and M. Takeda, *Mater. Sci. Eng. B Solid-State Mater. Adv. Technol.*, 2017, **219**, 20–27.

3 L. Cai, L. Song, P. Luan, Q. Zhang, N. Zhang, Q. Gao, D. Zhao, X. Zhang, M. Tu, F. Yang, W. Zhou, Q. Fan, J. Luo, W. Zhou, P. M. Ajayan and S. Xie, *Sci. Rep.*, 2013, **3**, 1–9.

4 J. Z. Gul, M. Sajid and K. H. Choi, *J. Mater. Chem. C*, , DOI:10.1039/c8tc03423k.

5 J. Luan, Q. Wang, X. Zheng, Y. Li and N. Wang, .

6 R. Iglio, S. Mariani, V. Robbiano, L. Strambini and G. Barillaro, *ACS Appl. Mater. Interfaces*, 2018, **10**, 13877–13885.

7 S. Xu, D. M. Vogt, W. H. Hsu, J. Osborne, T. Walsh, J. R. Foster, S. K. Sullivan, V. C. Smith, A. W. Rousing, E. C. Goldfield and R. J. Wood, *Adv. Funct. Mater.*, 2019, **29**, 1–14.

8 Y. Huang, Y. Zhao, W. Pan, Y. Zhang, X. Guo, L. Mao, P. Liu and L. Gao, *Smart Mater. Struct.*, 2017, **26**, 95017.

9 S. Zhu, J. H. So, R. Mays, S. Desai, W. R. Barnes, B. Pourdeyhimi and M. D. Dickey, *Adv. Funct. Mater.*, 2013, **23**, 2308–2314.

10 M. Xu, J. Qi, F. Li and Y. Zhang, *Nanoscale*, 2018, **10**, 5264–5271.

11 J. W. Lee, A. M. Soomro, M. Waqas, M. A. U. Khalid and K. H. Choi, *Int. J. Energy Res.*, 2020, **44**, 7035–7046.

12 X. Shi, C. H. Cheng, Y. Zheng and P. K. A. Wai, *J. Micromechanics Microengineering*, , DOI:10.1088/0960-1317/26/10/105020.

13 G. Hassan, J. Bae, A. Hassan, S. Ali, C. H. Lee and Y. Choi, *Compos. Part A Appl. Sci. Manuf.*, 2018, **107**, 519–528.

14 F. Jabbar, A. M. Soomro, J. Lee, M. Ali, Y. S. Kim, S. Lee and K. H. Choi, 2020, **32**, 1–17.